Nuclear Engineering and Design 254 (2013) 218–227

Contents lists available at SciVerse ScienceDirect

Nuclear Engineering and Design

journal homepage: www.elsevier.com/locate/nucengdes

Phenomenology involved in self-pressurized, natural circulation, low thermo-dynamic quality, nuclear reactors: The thermal–hydraulics of the CAREM-25 reactor

C.P. Marcel[a,b,c,*], H.F. Furci[a,b], D.F. Delmastro[a,b], V.P. Masson[b,c]

[a] Instituto Balseiro, 8400 S. C de Bariloche, Argentina
[b] Centro Atómico Bariloche, CNEA, Bustillo 9500, 8400 S. C. de Bariloche, Argentina
[c] Consejo Nacional de Investigaciones Científicas y Técnicas (CONICET), Argentina

HIGHLIGHTS

- Low quality, natural circulation, and self-pressurized nuclear reactors are modeled analytically.
- The feedbacks resulting from the interplay of the acting phenomena are analyzed.
- By decreasing the nuclear power the core inlet enthalpy increases.
- The mass flow has to be regulated to set it within a certain range in order.

ARTICLE INFO

Article history:
Received 9 June 2012
Received in revised form 9 August 2012
Accepted 27 September 2012

ABSTRACT

The interwoven phenomena involved in a prototypical self-pressurized natural circulation, low thermo-dynamical quality nuclear reactor such as CAREM-25 are analytically presented. These phenomena present many differences with traditional light water nuclear power plants. The dependence between mass flow and core inlet enthalpy on generated power is found. The need of tuning the mass flow rate in accordance to the design value is found to be important in order to keep the thermal margin and the heat transfer coefficients in the steam generators. The influence of condensation in structures or walls in the upper dome on the two-phase boundary is also studied. The dynamic consequences of all these results are therefore discussed. A numerical code is then used to verify the aforementioned findings and to test the validity of the modeling approximations. From the results it is clear that the way the phenomena interact causes the resulting dynamics in CAREM-25 to be substantially different from that existing in reactors such as PWRs, BWRs and also natural circulation BWRs. It is thus clear that the combination of different effects makes CAREM-25 behavior impossible to be extrapolated from existing knowledge and accumulated experience.

1. Introduction

Increases in nuclear power plant unit capacity have been promoted to take advantage of economies of scale while further enhancing safety and reliability. As a result, more than 400 units of nuclear power plants are playing an important role in electric power generation. Currently, the next generation nuclear reactors with ~1700 MWe are already available for construction. However, the future of nuclear power generation looks uncertain because of increasing competition with other sources of power generation in the deregulated market in spite of the fact that nuclear power generation is generally recognized as an attractive option from the viewpoints of energy security and environment protection. Furthermore, the factors, such as stagnant growth in the recent electricity demand, limitation in electricity grid capacity and the desire to minimize financial risk by limiting the initial investment, will not be in favor of large plant outputs. Nuclear power plants that can be easily adopted in any country are required in order to globalize nuclear power generation for greenhouse effect mitigation.

CAREM-25 is an Argentine project aimed to achieve the development, design and construction of an innovative, simple and small Nuclear Power Plant (NPP). This nuclear plant has an

* Corresponding author at: Centro Atómico Bariloche, CNEA, Bustillo 9500, 8400 S. C. de Bariloche, Argentina. Tel.: +54 2944 445101.
E-mail address: christian.marcel@cab.cnea.gov.ar (C.P. Marcel).

0029-5493/$ – see front matter © 2012 Elsevier B.V. All rights reserved.
http://dx.doi.org/10.1016/j.nucengdes.2012.09.005

Nomenclature

A	reference cross section in the loop (m^2)
C_P	heat capacity (kJ/kg)
D	diameter (m)
F	distributed friction coefficient
f	force (kg m/s^2)
g	gravity acceleration (m/s^2)
G	mass flux (kg/m^2 s)
h	enthalpy of the liquid (kJ/kg K)
k	localized friction coefficient
K	single friction coefficient
L	length (m)
$\dot{m}$	coolant flow in the circuit (kg/s)
P	pressure at the steam dome (Pa)
q	power flux (W/m^2)
Q	power (W)
T	temperature (K)
v	local fluid velocity (m/s)
z	refers to position within the loop (m)

Greek letters

β	expansion coefficient (1/K)
λ	flashing-boiling boundary length (m)
ρ	density (kg/m^3)
χ	thermo-dynamic equilibrium quality

Subscripts

0	reference value
Buoy	buoyancy
Cond	condensation in the steam dome
Ch	chimney section
Cr	critical
E	exit location
fg	liquid vapor phase change
fric	friction
I	inlet location
L	liquid at saturation
Nuc	core section
Sat	saturation
Sys	system, entrance of the cooled section
SG	steam generators
V	vapor at saturation

indirect cycle reactor with some distinctive and characteristic features which greatly simplify the design, and also contributes to a higher safety level. Some of the high-level design characteristics of the plant are: an integrated primary cooling system, natural circulation as the only mean of cooling the reactor core and self-pressurization of the primary system. The pressure value in CAREM-25 is achieved by balancing the vapor production in the core plus chimney sections (by means of boiling and flashing effect) and the condensation of vapor in contact with cold structures in the upper steam dome. The CAREM-25 concept was first presented in March 1984 in Lima, Peru, during the IAEA conference on small and medium size reactors. CAREM-25 was, chronologically, one of the first designs of the present new generation of reactor. The first step of this project is the construction of the prototype of about 27 MWe (CAREM-25). The design basis is supported by the cumulative experience acquired in research reactors design, construction and operation, and pressurized heavy water reactors (PHWR) nuclear power plants operation as well as the development of advanced design solutions (Gomez, 2000; IAEA, in press). CAREM-25 has been recognized as an International Near Term Deployment (INTD) reactor by the Generation IV International Forum (GIF).

The phenomenology of low quality natural circulation systems has been analyzed both in a theoretical and in an experimental way by several authors (Su et al., 2001, 2002; Marcel et al., 2009). Despite these valuable works, none of such investigations studied the case of self-pressurized systems as the one presented in the present article. In addition, different small integrated reactor designs exist, some of which are (partially) cooled by natural circulation low equilibrium quality flows, which phenomenology was extensively discussed in different works (Gou et al., 2006; Kusunoki et al., 2000; Iida et al., 1994; Lee et al., 2000). What makes CAREM-25 design different, however, is the fact it does not have any active system in order to control the system pressure. Due to this, the interwoven phenomena involved in CAREM-25 reactor promote a behavior which is different than that from other more traditional light water nuclear power plants (including the aforementioned designs). Such a difference has strong consequences in the reactor thermal–hydraulics as it has been pointed out in previous works (IAEA, in press; Delmastro, 2008). In this paper the thermal–hydraulic behavior of a natural circulation, low thermodynamic quality, self-pressurized, integrated reactor is thoroughly analyzed in both analytical and numerical ways.

2. The CAREM-25 reactor

CAREM-25 is an indirect cycle reactor with some distinctive features that greatly simplify the design and also contributes to a high safety level. Some of the high-level design characteristics are:

- Integrated primary cooling system (i.e. the primary circuit and the steam generators are located entirely within the reactor pressure vessel (RPV)).
- Self-pressurized.
- Natural circulation.
- Safety systems relying on passive features.

Despite these features, as an innovative reactor, the interactions between present phenomena need to be analyzed in depth in order to guarantee a safe operation in all range. In particular, this document deals with the basic thermal–hydraulic phenomenology present in the reactor and some parameters which may be of importance to the thermal–hydraulic stability.

2.1. Primary circuit and its main characteristics

The CAREM-25 nuclear power plant design is based on a light water integrated reactor. The whole high-energy primary system, core, steam generators, primary coolant and steam dome, is contained inside a single pressure vessel.

In CAREM-25 the flow rate in the reactor primary system is achieved by natural circulation. Fig. 1 shows a diagram of the natural circulation of the coolant in the primary system. Water enters the core from the lower plenum. After being heated, the coolant exits the core and flows up through the chimney to the upper dome. In the upper part, water leaves the chimney through lateral windows to the external region. It then flows down through modular steam generators, decreasing its enthalpy. Finally, the coolant exits the steam generators and flows down through the downcomer to the lower plenum, closing the circuit. The driving force obtained by the differences in the density along the circuit is balanced by the friction and form losses. In this way the adequate flow rate establishes in the core in order to have the sufficient thermal margin to critical phenomena. Coolant natural circulation is produced by the

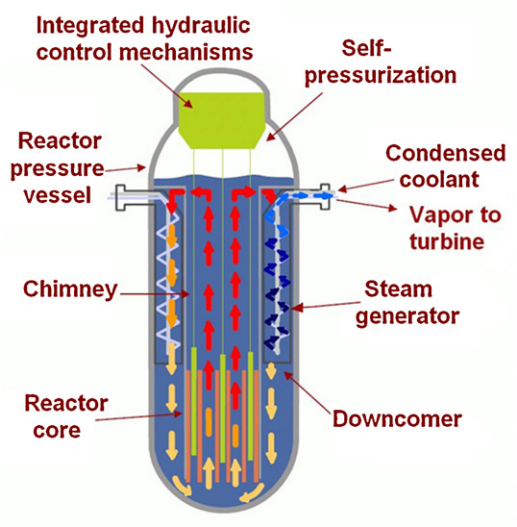

Design Name	CAREM-25
Reactor Type	Int. PWR
Thermal Power	100 MW(t)h
Electric Power	27 MW(e)
Fuel	LE UO_2
Cooling Mode	Nat. Circ.
Coolant Inventory	39 m3
Coolant mass flow	410 Kg/s
Operating Pressure	12.25 MPa
Core Inlet Temp.	284 °C
Core Outlet Temp.	326 °C
Core Length	1.4 m
Chimney Length	4.6 m
Steam Generator N°	12
Feed Water Temp.	200 °C
Steam Pressure	4.7 MPa

Fig. 1. The CAREM-25 reactor – schematic view of the flow circulation and general data.

location of the steam generators above the core. Coolant also acts as neutron moderator.

Self-pressurization of the primary system in the steam dome is the result of the liquid–vapor equilibrium. The large vapor volume in the RPV acting as an integral pressurizer, also contributes to the damping of eventual pressure perturbations. Due to self-pressurization, bulk temperature at core outlet corresponds to saturation temperature at primary pressure. In this way, typical heaters present in conventional PWRs are eliminated.

2.2. Primary components

Twelve identical 'Mini-helical' vertical steam generators, of the "once-through" type are placed equally distant from each other along the inner surface of the Reactor Pressure Vessel (RPV). They are used to transfer heat from the primary to the secondary circuit, producing superheated dry steam at 4.7 MPa. The secondary system circulates upwards *within the tubes*, while the primary coolant moves in counter-current flow. Due to the low liquid velocity in the upper plenum and the large cross sectional area for flow circulation, carry under is not considered to occur in the simplified analysis presented in this work.

In order to achieve a mostly uniform pressure-loss and superheating on the secondary side, the length of all tubes is equalized.

Due to safety reasons, the steam generators are designed to withstand the primary pressure without pressure in the secondary side and the whole live steam system is designed to withstand primary pressure up to isolation valves (including the steam outlet/water inlet headers) in case of SG tube breakage.

2.3. Operating characteristics

Different flow rates of coolant are produced in the primary system according to the power generated (and removed through the SG's). Numerical simulations have showed under different power transients a self-correcting response in the flow rate is obtained (Delmastro, 2000).

Due to the self-pressurizing of the RPV (steam dome) the system keeps the pressure very close to the saturation pressure. At all operating conditions this has proved to be sufficient to guarantee a remarkable stability of the RPV pressure response. The control system is capable of keeping the reactor pressure practically at the operating set point through different transients, even in case of power ramps.

The negative reactivity feedback coefficients and the large water inventory in the primary circuit combined with the self-pressurization features make this behavior possible with minimum control rod motion.

3. Phenomenology involved in the CAREM-25 reactor thermal–hydraulics

The physics involved in the CAREM-25 reactor includes different well known phenomena including self-pressurization, flashing, natural circulation, condensation, density wave instabilities, neutronic coupling, etc. The combination of these, however, creates numerous feedbacks which influence the reactor dynamics creating novel situations which are potentially destabilizing and therefore need to be investigated in depth (IAEA, in press).

In this paper, different aspects of the aforementioned phenomena which will contribute to the understanding of the CAREM-25 reactor behavior are described. In this analysis no subcooled boiling is assumed.

3.1. Single-phase natural circulation

In CAREM-25 reactor the steam quality is very low and therefore the largest contribution driving term in the momentum balance is due to single-phase buoyancy forces. In particular, in the simplified analysis developed in this section, the following assumptions are considered:

- Only single-phase natural circulation is considered.
- The Boussinesq approximation is considered to be valid.
- The heat flux is uniform regarding the axial direction.

The coolant flow in a natural circulation loop is driven by a difference in the density profile between the upwards and downwards legs of the circuit. Formally, the so-called buoyancy force can be defined in terms of the following integral along the circuit:

$$F_{buoy} = \oint A\rho_{(s)}g \cos\theta ds \quad (1)$$

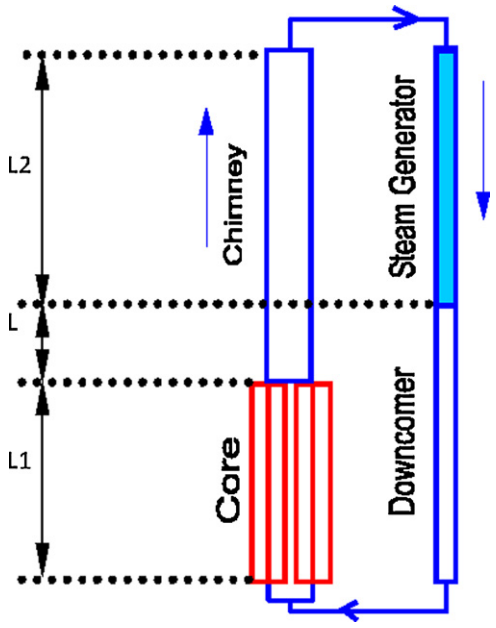

Fig. 2. Schematic of the considered closed circuit representing CAREM-25.

The integration variable s is a curvilinear coordinate along the circuit and θ is the angle formed by the versors $\check{s}$ and $\check{z}$, which correspond to the flow direction and the gravity, respectively.

In CAREM-25 reactor since the flow velocity and its derivative are very small at any condition, the inertial component of the pressure drop is negligible. Due to this, the pressure drop component which compensates the buoyancy force in the system is due to friction losses (including pressure losses due to flow path changes and secondary flows that are induced). The stationary condition is therefore reached when buoyancy forces are balanced with friction forces.

In order to estimate the flow rate it is necessary to estimate these two forces in terms of the relevant physical and geometrical magnitudes. To simplify such a calculation let us assume a closed loop in which only one phase is present, with a uniformly heated section placed at the bottom of the upwards branch and a uniformly cooled section located at the top of the downwards branch, with all other sections isolated (see Fig. 2).

The length of the heated and cooled sections is $L1$ and $L2$, respectively while L is the vertical distance existing between these two sections. A is the reference cross sectional area of the circuit. The buoyancy force for the steady state condition in this circuit is found by solving the integral in Eq. (1).

$$F_{buoy} = Ag[-\tilde{\rho}L_1 - \rho_l L - \rho_l L_2 + \tilde{\rho}L_2 + \rho_i L + \rho_i L_1] \tag{2}$$

where ρ_i and ρ_i are the fluid density at the inlet and outlet of the heated part, respectively and $\tilde{\rho}$ is the corresponding average. Eq. (2) can be rewritten as

$$F_{buoy} = A\Delta\rho g\left(L + \frac{L_1 + L_2}{2}\right) \tag{3}$$

where $\Delta\rho = \rho_i - \rho_l$

The total power Q_{Nuc} entering the system must be equal to the coolant enthalpy change in the core Δh times the mass flow rate $\dot{m}$, mathematically,

$$Q_{Nuc} = \dot{m}(h_{Nuc,e} - h_{Nuc,i}) = \dot{m}\Delta h = \dot{m}c_p\Delta T_{Nuc} \tag{4}$$

where the fluid temperature changes are related with density changes through the thermal expansion coefficient β: $\Delta\rho = \rho_l\beta\Delta R_{Nuc}$. For simplicity the Boussinesq approximation is assumed.

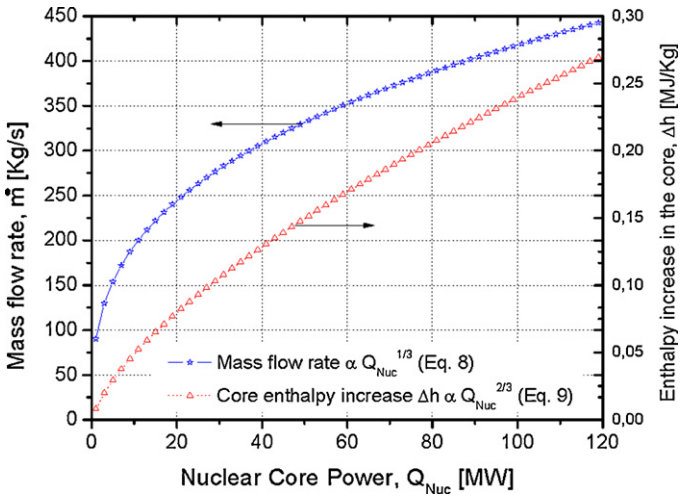

Fig. 3. The relation existing between the mass flow rate and the core power as predicted by Eq. (8) which is of the form $\dot{m} \propto Q_{Nuc}^{1/3}$. The figure also shows the enthalpy increase in the core as a function of the core power predicted by Eq. (9).

By replacing and operating it is easy to find the buoyancy force term.

$$\Delta\rho = Q_{Nuc}\frac{\beta}{\dot{m}c_p} \Rightarrow F_{buoy} = A\frac{Q_{Nuc}}{\dot{m}}\frac{g\beta\rho_l}{C_p}\left[L + \frac{L_1 + L_2}{2}\right] \tag{5}$$

The friction losses can be estimated as

$$F_{fric} = A\left[\underbrace{\sum f\frac{L}{2D}\rho v^2}_{\text{distributed}} + \underbrace{\sum\frac{1}{2}k\rho v^2}_{\text{concentrated}}\right] \equiv K\frac{\dot{m}^2}{2\rho_l A} \tag{6}$$

where v is the local velocity and f and k are distributed and concentrated friction factors, respectively. To simplify the analysis a single friction coefficient K is defined which condenses the two aforementioned effects and relates F_{frict} with $\dot{m}^2$.

The steady state condition is reached when:

$$A\frac{Q_{Nuc}}{\dot{m}}\frac{g\rho_l\beta}{c_p}\left[L + \frac{L1 + L2}{2}\right] = K\frac{\dot{m}^2}{2\rho_l A} \Rightarrow \dot{m}^3$$
$$= Q_{Nuc}\frac{2A^2g{\rho_l}^2\beta}{Kc_p}\left[L + \frac{L1 + L2}{2}\right] \tag{7}$$

Finally, it is possible to obtain the desired relation as (IAEA, in press)

$$\dot{m} = \sqrt[3]{\frac{2A^2Q_{Nuc}g{\rho_l}^2\beta}{Kc_p}\left[L + \frac{L1 + L2}{2}\right]} \tag{8}$$

From Eq. (8) it is clear the relation between the power and the mass flow rate is not linear.

By using Eqs. (8) and (4) the enthalpy increase in the core section can be obtained.

$$h_{Nuc,e} - h_{Nuc,i} = \Delta h = \frac{Q_{Nuc}}{\dot{m}} = \sqrt[3]{\frac{Kc_pQ_{Nuc}^2}{2A^2g{\rho_l}^2\beta}\left[L + \frac{L1 + L2}{2}\right]^{-1}} \tag{9}$$

In order to clarify the relations given by Eqs. (8) and (9), Fig. 3 is constructed by using typical CAREM-25 values at rated conditions.

3.2. The self-pressurization mechanism

In order to have a constant pressure during CAREM-25 normal operation, some vapor needs to be created inside the RPV. Let us assume for a while, the vapor generation rate is larger than the condensation rate. Under such a condition, the saturation enthalpy of

the liquid increases, decreasing the vapor generation rate, which in turn decreases the system pressure. In addition to this effect, the condensation rate is also expected to increase due to the increase in the fluid saturation temperature. Such feedback mechanisms therefore tend to maintain the pressure constant.

Assuming that no carry under is present, the vapor generated in the hot leg of the circuit is condensed before entering the cooling devices.

The heat losses occurring in the reactor pressure vessel (except the steam dome) are much smaller than the rest of the power terms involved in the system and therefore they can be neglected.

In this way, the energy balance for the entire circuit at steady state yields

$$Q_{Nuc} = Q_{SG} + Q_{Cond} \tag{10}$$

where Q_{SG} is the power extracted by the cooling devices (i.e. the steam generators) and being Q_{Cond} the power related with vapor condensation. It needs to be emphasized that for most conditions $Q_{Nuc} \gg Q_{Cond}$.

The heat balances in the heated and cooled sections yield

$$Q_{Nuc} = \dot{m}(h_{Nuc,e} - h_{Nuc,i}) \tag{11a}$$

$$Q_{SG} = \dot{m}(h_{sat} - h_{SG,e}) = \dot{m}(h_{sat} - h_{Nuc,i}) \tag{11b}$$

By replacing Eqs. (11) into (10) we finally obtain an expression for the condensation power Q_{Cond}:

$$Q_{Cond} = \dot{m}(h_{Nuc,e} - h_{sat}) \tag{12}$$

Such a condensation takes place in the upper part of the reactor and is a direct consequence of the heat losses and the interaction of the vapor with cold structures present in the steam dome such as those from the reactivity control mechanism.

Eq. (9) combined with Eqs. (12) and (8) can be used to find an expression for the core inlet enthalpy $h_{Nuc,i}$,

$$h_{Nuc,i} = h_{sat} - (Q_{Nuc} - Q_{Cond}) \sqrt[3]{\frac{Kc_p}{2A^2 Q_{Nuc} g \rho_l{}^2 \beta} \left[L + \frac{L1 + L2}{2}\right]^{-1}} \tag{13}$$

From this result it can be observed that in a self-pressurized, natural circulation such as CAREM-25, the core inlet enthalpy cannot be controlled directly but it is a result of the combination of the produced and condensed power in the system.

Eq. (9) can be used to calculate the mean enthalpy in the reactor core, $\bar{h}_{Nuc}$, thus

$$\bar{h}_{Nuc} = \frac{h_{Nuc,e} + h_{Nuc,i}}{2} = \frac{1}{2} \sqrt[3]{\frac{Kc_p {Q_{Nuc}}^2}{2A^2 g \rho_l{}^2 \beta} \left[L + \frac{L1 + L2}{2}\right]^{-1}} + h_{Nuc,i} \tag{14}$$

Replacing Eq. (13) into Eq. (14) the mean core enthalpy is obtained in terms of the produced and condensed powers.

$$\bar{h}_{Nuc} = h_{sat} - \left(\frac{Q_{Nuc}}{2} - Q_{Cond}\right) \sqrt[3]{\frac{Kc_p}{2A^2 Q_{Nuc} g \rho_l{}^2 \beta} \left[L + \frac{L1 + L2}{2}\right]^{-1}} \tag{15}$$

For CAREM-25 conditions ($Q_{Nuc} \gg Q_{Cond}$) Eq. (15) indicates that when decreasing the power level while maintaining all other parameters constant, the mean enthalpy in the core approaches to the saturation value, which indicates the core is hotter at low power levels than at nominal condition. This result is quite anti-intuitive and reveals a different behavior of CAREM-25 reactor compared to conventional nuclear pressurized water reactors (PWRs). In such reactors, a lower power level is associated to a lower value of the core enthalpy exit while the core inlet enthalpy is roughly constant. In CAREM-25 reactor the core exit enthalpy is very close to the saturation enthalpy at all conditions and a lower power level is associated to a *higher* core inlet enthalpy.

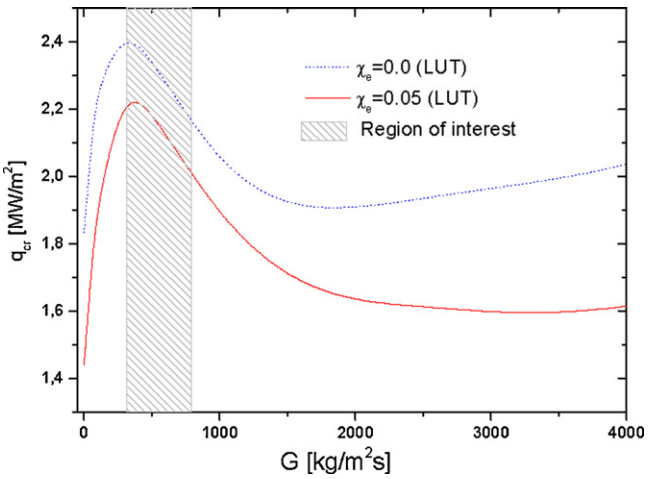

Fig. 4. Critical heat flux vs. mass flux for two different thermo-dynamical qualities obtained from the Lookup Tables. The region of interest for CAREM-25 reactor operating at nominal condition is also showed.

3.3. Limitations in the coolant mass flow rate

In a self-pressurized, natural circulation reactor such as CAREM-25, the uncertainties related to the prediction of the resulting coolant mass flow rate need to be carefully studied. In particular, two extreme cases might occur (IAEA, in press):

(a) The total friction in the system might be overestimated.
(b) The total friction in the system might be underestimated.

In case (a) if K is overestimated it might happen that friction in reality is much smaller than estimated. This could have undesired consequences from the thermal margin point of view and deserves a special attention.

It is well known that two of the most crucial parameters influencing the critical heat flux (CHF) are the local quality χ and the mass flux G flowing through the channel.

The CAREM reactor operates in a particular region of the critical heat flux, q_{cr} vs. G curve which is characterized by the fact when increasing the mass flux G, the critical power is decreased. In order to clarify this behavior, the following figure, for relevant CAREM conditions, is constructed by using the Lookup Tables 1986 (LUT) (Groeneveld et al., 1986). Although such a trend is not fully understood, the most accepted explanation is as follows. At low mass flux the bubble dynamics is driven by buoyancy and the bubbles tend to go faster than the liquid. Near the wall, where there is a significant liquid velocity gradient, the bubbles flow faster than the liquid, which results in bubble rotation which in turn gives a lateral force to the bubbles away from the wall (which enhances the CHF). At higher velocities, where buoyancy becomes less important, the bubble velocity lags that of the liquid. In the near wall region, where the velocity gradient is largest, the velocity gradient again results in a bubble rotation but this time the bubbles rotational velocity is opposite to the case where buoyancy dominates. As a result the bubbles want to move toward the wall, which will result in bubble clouding effect, which lowers the CHF (Groeneveld, 2012).

Fig. 4 also shows that when increasing the local quality χ the critical heat flux q_{cr} decreases.

In CAREM reactor the mean thermodynamic quality in the reactor core can be used to characterize the occurrence of critical heat

flux. Eqs. (8) and (15) can be used to find the mass flux G, and the mean quality in the core $\bar{\chi}$ respectively, resulting:

$$G = \sqrt[3]{\frac{2Q_{Nuc} g \rho_l^2 \beta}{AKc_p}\left[L + \frac{L1+L2}{2}\right]} \tag{16}$$

$$\bar{\chi} = \frac{-Q_{Nuc} + 2Q_{Cond}}{2h_{fg}} \sqrt[3]{\frac{Kc_p[2L+L1+L2]^{-1}}{4A^2 Q_{Nuc} g \rho_l^2 \beta}}$$
$$\approx \frac{-Q_{Nuc}^{2/3}}{2h_{fg}} \sqrt[3]{\frac{Kc_p[2L+L1+L2]^{-1}}{4A^2 g \rho_l^2 \beta}} \tag{17}$$

From Eqs. (16) and (17) it is clear that if the real friction in the system is lower than the estimated value (represented by the factor K), both, the mass flux and the mean quality increases (i.e. the mean quality becomes less negative), causing the thermal margin to reduce. For this reason it is of great importance to fix a maximum mass flow rate in CAREM reactor.

In case (b) on the contrary, if the friction is largely underestimated, the resulting mass flow rate will be smaller than expected. This might imply the steam generators need to be able to cool down the flow beyond the designed values (see Eq. (11b)). It may therefore occur that the steam generators are not able to evacuate the prescribed power.

From this simple analysis it is clear that for a given power the mass flow rate must remain in a certain range in order to avoid any undesired consequence in the system. In order to eliminate deviations of the obtained mass flow rate regarding the design value, special pressure drop devices located at the core inlet location will be adjusted during commissioning of the reactor.

3.4. Density wave instabilities

The highly complex phenomena occurring in nuclear reactors cooled by two-phase flows have motivated extensive research programs in the past with a strong emphasis in stability studies. As a result of these, important knowledge has been generated which helped to understand the main instability mechanisms. For instance, it is known that the most important instabilities in currently operating Boiling Water Reactors (BWRs) are purely thermal–hydraulic and coupled neutronic–thermal–hydraulic instabilities (Bouré et al., 1973; Lahey and Moody, 1979). These instability types are basically induced by the 'density-wave' character of the two-phase flow in the coolant channels.

It is usual to divide the density wave oscillations (DWOs) into two main instability types: Type-I instabilities induced by the gravitational pressure drop term, and Type-II instabilities due to frictional pressure losses.

The Type-I instability mechanism usually becomes dominant in natural circulation reactors operating at low quality flows, e.g. during BWRs start-up and in novel reactors such as CAREM-25. Under these conditions, the mass percentage of steam, i.e. the flow quality, at the core exit becomes very small. For small flow qualities (and particularly at low pressures) the volumetric amount of steam (the void fraction) increases very rapidly as a function of the flow quality. A small decrease in the core inlet flow then leads to a large increase of the volume of steam produced at the core exit. In a natural circulation reactor, this causes a low-density wave traveling through the chimney. This enhances the driving head, and the inlet flow therefore increases. Then the opposite process occurs, and the void fraction in the chimney decreases. Consequently, the driving head becomes smaller, and the flow rate therefore decreases. This completes one cycle of a Type-I oscillation. The main time constant governing this type of DWO is the transit time of the voids through the chimney section (~5 to 15 s) (Fukuda and Kobori, 1979; Marcel, 2007; Marcel et al., 2008 Nov).

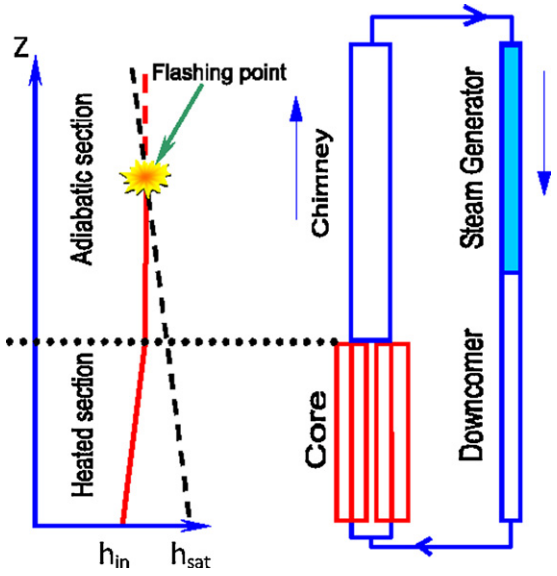

Fig. 5. Schematic of a CAREM-25 reactor and the occurrence of flashing.

3.5. The flashing phenomenon

In CAREM-25, besides some vapor created in the core (the vapor quality at the exit of such a section is practically zero), an important amount of vapor is created by the so-called flashing phenomenon occurring in the chimney.

The natural circulation CAREM-25 reactor can be represented as a loop, (see Fig. 5), with a cold section (the downcomer), a heated section (the core), an adiabatic section (the chimney) and a heat exchanger. As shown before, density differences between the cold and hot legs cause the water to flow without using pumps. Natural circulation is thus enhanced in this type of reactor by using a tall chimney.

As the heated coolant flows upwards, the hydrostatic pressure will decrease. Hence, the saturation temperature will also decrease. If the saturation enthalpy becomes equal to the (constant) fluid enthalpy in the chimney, vapor creation by flashing occurs – i.e. boiling out of the heated reactor core (see Fig. 5). This ex-core boiling is enhanced as the reactor pressure decreases because at lower pressure the saturation enthalpy is more dependent of the axial position. In the particular case of the CAREM-25 reactor the flashing phenomenon is crucial for the stability analysis in both, the reactor start-up, i.e. at low pressure, and at nominal conditions. This is due to the fact the most unstable mode is due to low quality density waves traveling through the reactor chimney in which the vapor creation in this section is of great importance.

Let us add the flashing mechanism to the closed loop model described previously.

The fluid entering the cooling section (representing the steam generators) is assumed to be saturated. In addition, the coolant leaves such a section (i.e. it enters the heated section) with an enthalpy $h_{Nuc,i}$. The enthalpy of the fluid leaving the reactor core is $h_{Nuc,e}$.

Pressure in the system will vary along the vertical direction due to the hydrostatic pressure decrease and friction losses (the acceleration and inertial contributions are small and thus not considered). Let us call P_{Sys} the pressure at the highest part of the circuit which coincides with the pressure at the entrance of the cooled section. Neglecting the friction contribution in the chimney section (which

represents less than 5% of the total pressure drop), the pressure as a function of the axial location is given by

$$P(z) = P_{Sys} + \rho_l g z \tag{18}$$

where z is the distance from the top of the heated section. As can be noted the density is assumed constant along the hot leg above the heated section. This axial pressure variation causes a variation of the saturation enthalpy along z. This can be expressed as

$$h_{Sat}(z) = h_{Sat}(P(z)) = h_{Sat}(P_{Sys} + \rho g z) \tag{19}$$

Taking a first order approximation in the enthalpy variation

$$h_{sat}(z) = h_{Sat}(P_{Sys}) + \left.\frac{\partial h_{Sat}}{\partial P}\right|_{P=P_{Sys}} \rho_l g z \tag{20}$$

The onset of flashing will take place at the value of $z = \lambda$ in the hot leg that satisfies the following equality

$$h_{Sat}(\lambda) = h_{Nuc,e} \tag{21}$$

with λ being the flashing boundary measured from the chimney top. The condition that the fluid is at saturation point at the entrance of the cooled section has certain implications. Since no carry under of bubbles is present, all vapor needs to be condensed *before* entering the cooled section. Such phenomenon occurs in CAREM-25 reactor in the upper dome zone. In other words, the excess of enthalpy over the saturation value (at the chimney exit) is evacuated through condensation in the steam dome walls or other structures of the vapor originated by flashing (and boiling, if present). It is assumed that the mass of condensed fluid in the dome flows back into the liquid region at saturation enthalpy. The fluid which remains liquid during flashing is also assumed to be at saturation condition at local pressure.

The energy balance for the entire circuit at steady state, as presented before is thus modified accordingly.

$$Q_{Nuc} = Q_{SG} + Q_{Cond} \tag{22}$$

The heat balances in the heated and cooled sections are now

$$Q_{Nuc} = \dot{m}(h_{Nuc,e} - h_{Nuc,i}) \tag{23a}$$

$$Q_{SG} = \dot{m}(h_{Sat}(P_{Sys}) - h_{SG,e}) = \dot{m}(h_{Sat}(P_{Sys}) - h_{Nuc,i}) \tag{23b}$$

By replacing Eqs. (23) into (22) we obtain an expression for the condensation power Q_{cond} in the case the flashing effect is considered.

$$Q_{Cond} = \dot{m}(h_{Nuc,e} - h_{Sat}(P_{Sys})) \tag{24}$$

We can now use Eqs. (20), (21) and (24) to evaluate the point at which flashing starts:

$$\lambda = \frac{Q_{Cond}}{\dot{m}} \frac{1}{\rho_l g\, \partial h_{Sat}/\partial P\big|_{P=P_{Sys}}} \tag{25}$$

Although Eq. (8) neglects the two-phase contribution in the buoyancy force, it can be used for describing the mass flow rate with reasonable accuracy, as it is shown in a further section. By using such a relation, Eq. (25) is transformed into

$$\lambda = \frac{Q_{Cond}}{(\partial h_{Sat}/\partial P)\big|_{P=P_{Sys}}} \sqrt[3]{\frac{Kc_p}{2A^2 Q_{Nuc} g^4 \rho_l{}^5 \beta [L + ((L1 + L2)/2)]}} \tag{26}$$

As it can be observed, the flashing boundary position λ (measured from the top of the chimney) has a proportional relation with the condensation power Q_{Cond} and the inverse of the cubic root of the core power Q_{Nuc} (IAEA, in press). The reason for this is due to the fact by increasing Q_{Cond} the system has to generate more vapor in order to satisfy both constrains: keeping the pressure constant and avoiding carry under of bubbles in the steam generators. The mechanism for this is the following: when Q_{Cond} is increased the pressure tends to decrease since the condensation rate in the steam dome increases resulting in a smaller amount of vapor in the system. Such pressure reduction decreases the vaporization enthalpy in the system and therefore the flashing boundary tends to move downwards. Since more vapor is present in the system, the pressure increases until the pressure is reestablished to its original value. In other words, the reduction in the amount of vapor in the steam dome has to be compensated by an increase of vapor in the chimney, which starts to boil at lower locations. In the order to emphasize such a result, the following figure is constructed (Fig. 6).

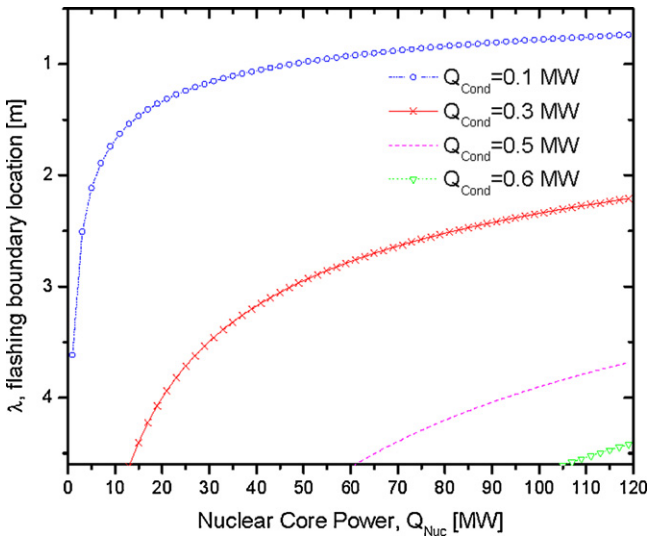

Fig. 6. Location of the flashing boundary measured from the chimney top at different reactor power levels, according to Eq. (26).

Eq. (26) has important implications: It is well known that the location of the boiling–flashing boundary has a strong effect in the void transport gain and delay which is the basis of density wave instabilities mechanism. The importance of the boiling-flashing boundary location is therefore obvious (note that when vapor is only produced in the chimney we refer to *the flashing boundary*, however in general we use the term *boiling–flashing boundary*). From the aforementioned equation, it can be seen that a possible way of *varying* the stability performance of the system (for a large range of core powers) is by changing the condensation power in the steam dome. In other words, the condensation power seems to be a very efficient means for varying the phase lag of the density waves traveling through the system and therefore can be used for stabilizing purposes.

To give an idea of the importance of this effect in the CAREM-25 case, a simple calculation is presented with which the amount of power involved in the flashing phenomena is estimated. Let us assume the reactor is working at nominal conditions and the core exit thermo-dynamic quality is zero, i.e. the coolant is saturated there.

Table 1
CAREM-25 reference values at nominal conditions with $\chi_e = 0$.

	Symbol [unit]	Chimney inlet	Chimney outlet
Position	Z (m)	0	4.6
Hydrostatic pressure	P [MPa]	12.25	12.22
Liquid density	ρ [kg/m^3]	651.0	651.5
Saturation temperature	T_{Sat} [°C]	326.26	326.07
Liquid enthalpy	h [kJ/kg]	1501.5	1500.3
Mass flow rate	$\dot{m}$	410	410

By using data from Table 1, the amount of power converted into vapor by means of the flashing phenomenon Q_{Cond} can be estimated as,

$$Q_{Cond} = \dot{m}(h_{Sat,Ch,i} - h_{Sat,Ch,e}) = 0.5\,\text{MW} \quad (27)$$

Thus, since the coolant is saturated at the core exit i.e. the chimney inlet, the flashing phenomenon provides vapor in the steam dome carrying a power equal to 0.5 MW. As mentioned before, such amount of vapor is separated in the free region located above the chimney and condensed in the dome and in the surface of the control mechanisms. Due to the large area for the void separation and the low coolant velocities, it is expected no or small carry under of bubbles will take place.

Vapor production in the chimney directly affects the gravitational pressure drop over this section. Hence, it can be expected that the Type-I feedback mechanism is amplified by the occurrence of void flashing, especially in natural circulation reactors with a tall chimney section such as CAREM-25.

3.6. The natural variables of the system

From the derived relations from previous sections it can be noted all the relevant parameters identifying the status of the reactor (e.g. the mass flow rate, the core inlet enthalpy, the core mean quality, the location of the boiling–flashing boundary, see Eqs. (8), (13), (17) and (26)), can be expressed by using geometrical parameters and three system variables. For convenience the selected three variables, so-called natural variables, are:

- The system pressure, P_{Sys} (defined at the steam dome) which basically influences the fluid properties and the saturation enthalpy variation with the pressure.
- The nuclear core power, Q_{Nuc}.
- The power which is condensed in the steam dome, Q_{Cond}.

4. The CAREM-25 behavior at steady state nominal conditions

The following results are obtained by means of the HUARPE code, which is a lowly diffusive numerical code specially developed to investigate CAREM-25 thermal–hydraulics aspects (see Zanocco et al., 2004a,b, for further details). It needs to be pointed out that in this work; the core inlet friction is adjusted in the code until the prescribed mass flow rate is obtained at rated conditions.

4.1. The coolant flow vs. power curve

In order to assess the behavior of the natural circulation in CAREM-25 reactor, the HUARPE code is used to calculate the coolant mass flow rate obtained for different nuclear core power levels when operating the reactor at nominal pressure and at a condensation power value equal to 0.5 MW. The resulting relation is presented in Fig. 7. For completeness, the relation between these two parameters predicted by Eq. (8) is also included.

As it can be observed in the figure, the mass flow rate as estimated with the numerical code shows a good agreement with the relation given by Eq. (8). It can be noted, however, the result from the HUARPE code predicts a higher mass flow rate than the explicit relation at low nuclear core power levels. This difference is explained by the fact that the condensation power (which is kept constant in this analysis) in this case is relatively high regarding to the core power. A relatively high condensation power causes the flashing boundary position to move downwards which enhances the two-phase contribution in the momentum balance (see Eq. (26)), which is not considered in the simplified model from which Eq. (8) is derived.

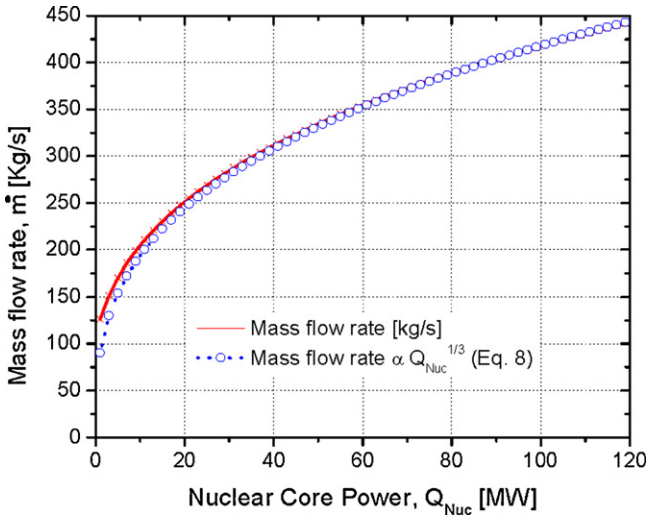

Fig. 7. The relation between the mass flow rate and the core power obeys a relation given by Eq. (8) which is of the form $\dot{m} \propto Q_{Nuc}^{1/3}$.

4.2. The coolant density profile along the reactor

In this section the coolant density profile along the reactor circulation coolant path is shown, see Fig. 8.

It needs to be mentioned that different correlations are used in order to estimate the heat transfer in the SGs according to the corresponding mechanism in the SGs secondary side: single-phase (overheated steam), nucleation or single-phase (subcooled) mechanism.

From the figure it can be seen the density decreases linearly in the reactor core and remains at a small value in the chimney (IAEA, in press). As the coolant enters the steam generators it is cooled showing a density increase which is more or less linear. The density remains at a large value until it enters the core section, closing the cycle. The dashed area from Fig. 8 is proportional to the buoyancy force driving the coolant.

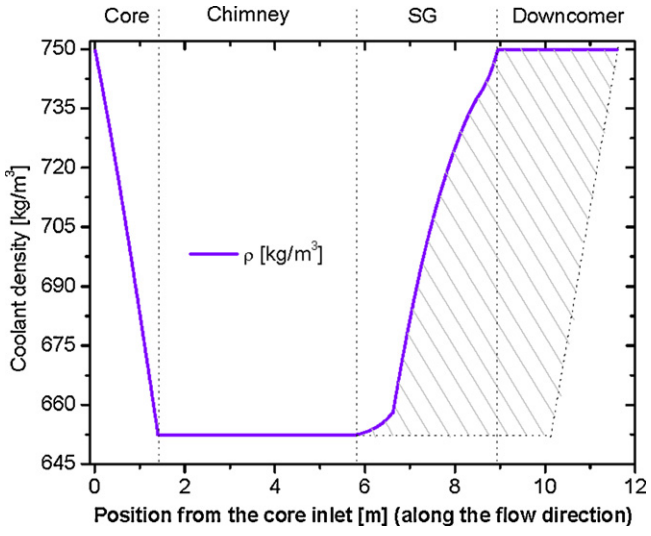

Fig. 8. The coolant density profile along the CAREM-25 primary circuit.

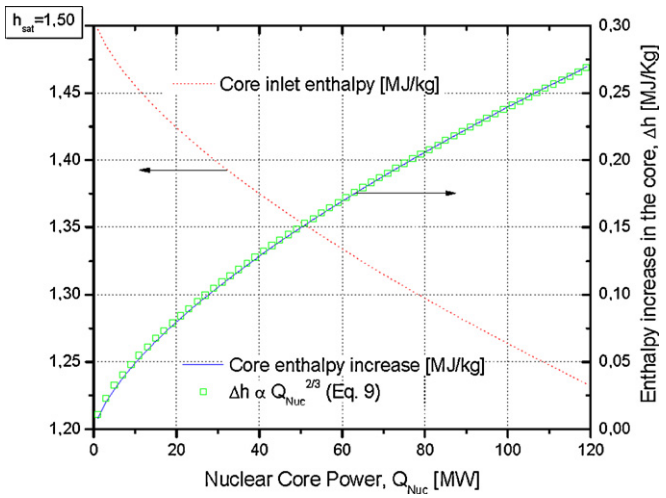

Fig. 9. Evolution of the enthalpy increase in the core section. The relation between Δh and the core power obeys a relation given by Eq. (9) which is of the form $\Delta h \propto Q_{Nuc}^{2/3}$.

4.3. The core enthalpy increase

In this section, HUARPE code is used to investigate the evolution of the core inlet enthalpy and also the enthalpy increase in the core when the system core power is varied. As in previous cases, the reactor is operated at nominal pressure and at a condensation power level equal to 0.5 MW. The result of this numerical experiment is shown in Fig. 9.

As can be seen from the figure, the core inlet enthalpy *increases* when decreasing the core power. In addition, the enthalpy increase in the core reduces when the power level decreases. This is explained by the fact the core outlet enthalpy is at any condition very close to the saturation value which implies the enthalpy at the core inlet has to increase when the power level decreases in order to satisfy Eq. (13).

This result is directly related with the self-pressurization mechanism which *fixes* the value of the core outlet enthalpy since vapor needs to be produced in order to maintain the system pressure. This behavior is different from other nuclear reactors for which the enthalpy at the core inlet is roughly fixed and the core exit enthalpy *follows* the power variations (Rohde et al., 2010).

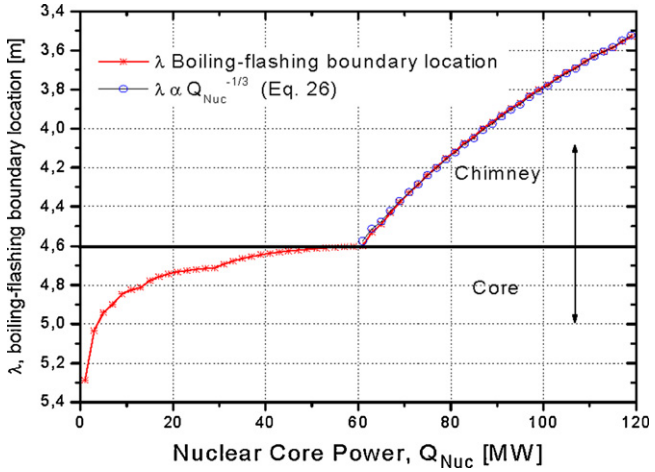

Fig. 10. The boiling–flashing boundary location estimated at different reactor power levels.

4.4. The boiling boundary location

As mentioned before, a very important parameter for stability analysis regarding density wave oscillations is the location of the boiling–flashing boundary in the system. Due to this, the following figure corresponding to CAREM-25 reactor operated at nominal pressure is constructed at a condensation power level equal to 0.5 MW and at different core power levels (Fig. 10).

From the figure it is seen that the boiling-flashing boundary location moves downwards as core power levels decrease. In particular, when there is no vapor production by means of boiling, the result is in agreement with the relation given by Eq. (26).

5. Conclusions

From the results shown in this work it is clear that the thermal–hydraulics governing self-pressurized, natural circulation reactors such as CAREM-25 is different from PWRs and also natural circulation BWRs. It is thus clear that the combination of different effects makes CAREM-25 behavior impossible to be extrapolated from existing knowledge and accumulated experience. Therefore an exhaustive analysis regarding the thermal–hydraulic performance (including stability analysis) needs to be performed. Summarizing, the following statements can be drawn from the CAREM-25 steady state results:

- Single-phase natural circulation is the most important driving mechanism in the reactor, which states the mass flow rate is proportional to the cubic root of the generated power.
- When operating CAREM-25 with a prescribed condensation power and pressure levels, the boiling-flashing boundary location occurs lower in the chimney for lower core power level.
- Unlike most nuclear reactors, in CAREM-25 the core inlet enthalpy increases when decreasing the core power.
- Unlike NC-BWRs, the self-pressurization phenomenon does not allow to directly control the coolant enthalpy at the CAREM-25 core inlet.
- The condensation power has a great impact in the boiling-flashing boundary location and thus it may influence the stability of CAREM-25. For this reason this variable is an optimal candidate for optimizing the stability performance of the reactor.
- Since the mass flow rate needs to be as close as possible to the designed value, a strategy like BWR assembly inlet orificing is to be used in CAREM-25 reactor.

References

Bouré, J.A., Bergles, A.E., Tong, L.S., 1973. Review of two-phase flow instability. Nucl. Eng. Des. 25 (165), p.165–p.192.
Delmastro, D., 2000. Thermal–hydraulic aspects of CAREM reactor. In: IAEA TCM on Natural Circulation Data and Methods for Innovative Nuclear Power Plant Design, Vienna, Austria.
Delmastro, D., 2008. Thermal–hydraulic aspects of self-pressurized natural circulation integral reactors. In: Proc. of International Workshop on Thermal–Hydraulics of Innovative Reactor and Transmutation Systems – THIRS, April 14–16, Eggenstein-Leopoldshafen, Germany.
Fukuda, K., Kobori, T., 1979. Classification of two-phase instability by density wave oscillation model. J. Nucl. Sci. Technol. 16 (2), 95–108.
Gomez, S., 2000. Development activities on advanced LWR designs in Argentina. In: Technical Committee Meeting on Performance of Operating and Advanced Light Water Reactor Designs, Munich Germany. IAEA Publications, pp. 113–120.
Gou, J., Qiu, S., Su, G., Jia, D., 2006. Theoretical investigation on the steady state natural circulation characteristics of a new type of pressurized water reactor. Nucl. Sci. Tech. 17 (5), 314–320.
Groeneveld, D.C., 2012. Personal communication.
Groeneveld, D.C., Cheng, S.C., Doan, T., 1986. 1986 AECL – UO critical heat flux Lookup Table. Heat Transfer Eng. 7 (1), 46–62.
International Atomic Energy Agency (IAEA). Advanced Water Cooled Reactor Case Studies in Support of Passive Safety Systems. IAEA-TECDOC, IAEA, Vienna, in press.

Iida, H., Ishizaka, Y., Kim, Y.-C., Yamaguchi, C., 1994. Design study of the deep-sea reactor X. Nucl. Tech. 107, 38–48.
Kusunoki, T., Olano, N., Yoritsune, T., Ishida, T., Hoshi, T., Sako, K., 2000. Design of advanced integral-type marine reactor MRX. Nucl. Eng. Des. 201 (2), 155–175.
Lahey Jr., R.T., Moody, F.J., 1979. The Thermal–Hydraulics of a Boiling Water Nuclear Reactor. American Nuclear Society, LaGrange Park, IL.
Lee, D.J., et al., 2000. Design and safety of a small integral reactor (SMART). In: Proc. Int. Workshop on Utilization of Nuclear Power in Oceans, February 21–24, Tokyo, Japan, pp. 23–31.
Marcel, C.P., 2007. Experimental and Numerical Stability Investigations on Natural Circulation Boiling Water Reactors. IOS press, The Netherlands.
Marcel, C.P., Rohde, M., Van der Hagen, T.H.J.J., 2008 Nov. Experimental Investigations on the ESBWR stability performance. Nucl. Technol. 164 (2), 232–244.
Marcel, C.P., Rohde, M., Van Der Hagen, T.H.J.J., 2009. Experimental and numerical investigations on flashing-induced instabilities in a single channel. Exp. Therm. Fluid Sci. 33, 1197–1208.
Rohde, M., Marcel, C.P., Van der Hagen, T.H.J.J., Manera, A., Shiralkar, B., 2010. Investigating the ESBWR stability with experimental and numerical tools: a comparative study. Nucl. Eng. Des. 240 (2), 375–384.
Su, G., Jia, D., Kenji, F., Guo, Y., 2001. Theoretical study on density wave oscillation of two phase natural circulation under low quality conditions. J. Nucl. Sci. Technol. 38 (8), 607.
Su, G., Jia, D., Kenji, F., Guo, Y., 2002. Theoretical and experimental study on density wave oscillation of two-phase natural circulation of low equilibrium quality. Nucl. Eng. Des. 215, 187–198.
Zanocco, P., Giménez, M., Delmastro, D., 2004a. Modeling aspects in linear stability analysis of a self-pressurized natural circulation integral reactor. Nucl. Eng. Des. 231, 283–301.
Zanocco, P., Delmastro, D., Giménez, M., 2004b. Linear and nonlinear stability analysis of a self-pressurized, natural circulation, integral reactor. In: ICONE12, International Conference on Nuclear Engineering, Washington, DC.